Highly under-coordinated atoms at Rh surfaces: interplay of strain and coordination effects on core level shift

2007 New J. Phys. 9 143

(http://iopscience.iop.org/1367-2630/9/5/143)

New Journal of Physics
The open-access journal for physics

Highly under-coordinated atoms at Rh surfaces: interplay of strain and coordination effects on core level shift

A Baraldi[1,2,6], L Bianchettin[1,2], E Vesselli[1,2], S de Gironcoli[3], S Lizzit[4], L Petaccia[4], G Zampieri[5,7], G Comelli[1,2] and R Rosei[1,2]

[1] Physics Department and Centre of Excellence for Nanostructured Materials, Trieste University, Via Valerio 2, I-34127 Trieste, Italy
[2] Laboratorio TASC INFM-CNR SS 14 Km 163.5, I-34012 Trieste, Italy
[3] SISSA—Scuola Internazionale Superiore di Studi Avanzati and INFM-CNR DEMOCRITOS National Simulation Centre via Beirut 2-4, I-34014 Trieste, Italy
[4] Sincrotrone Trieste SCpA SS 14 Km 163.5, I-34012 Trieste, Italy
[5] Centro Atómico Bariloche AR-8400 Bariloche, Argentina
E-mail: alessandro.baraldi@elettra.trieste.it

New Journal of Physics **9** (2007) 143
Received 12 December 2006
Published 21 May 2007
Online at http://www.njp.org/
doi:10.1088/1367-2630/9/5/143

Abstract. The electronic structure of highly under-coordinated Rh atoms, namely adatoms and ad-dimers, on homo-metallic surfaces has been probed by combining high-energy resolution core level photoelectron spectroscopy and density functional theory calculations. The $Rh3d_{5/2}$ core level shifts are shown to be proportional to the number of Rh nearest-neighbours ($n = 3$, 4 and 5). A more refined analysis shows that the energy position of the different core level components is correlated with the calculated changes of the individual inter-atomic bond length and to the energy changes of the d-band centre, which is known to be a reliable descriptor of local chemical reactivity.

[6] Author to whom any correspondence should be addressed.
[7] GZ is also member of CONICET, Argentina.

PII: S1367-2630(07)39149-0

Contents

1. Introduction

Atomic-level understanding of the physical properties of transition metal (TM) clusters and nanostructured surfaces outermost atomic layers, is a very important issue in condensed matter science. Both the reduced number of nearest-neighbours and the interatomic distance modifications (with respect to bulk or flat-surface geometries) strongly affect magnetic [1] and chemical properties [2], in a way that may meet emerging needs in technological fields, such as magnetic data storage and heterogeneous catalysis.

When TM atoms undergo reduced coordination and/or bond compressive or tensile strain, the overlap of d states at neighbouring sites changes, leading in turn, to changes in d to sp promotion or hybridization. While changing coordination numbers and lattice constants in a theoretical calculation is relatively simple, measuring electronic structure-related properties of under-coordinated monometallic structures, and making correlations with their atomic-level geometrical properties, is a much more demanding task, as experimental results are in general averaged over a large number of different local configurations [3]–[5].

The problem of understanding local properties becomes especially important in systems with a large number of highly under-coordinated atoms like small atomic aggregates or nanostructured surfaces. For example a strong reduction in the activation barrier of chemical reactions at low coordinated reaction centres has been found in the case of stepped surfaces [6]–[14]. Moreover at elevated temperatures, even an appreciable concentration of atoms with very low coordination (e.g. adatoms evaporated from kink sites at steps), has been proven to exist on many material surfaces [15]–[17]. Adatoms have been found to play a crucial role in determining reaction pathways in a number of catalytic processes [18]–[22]. The possibility of obtaining direct experimental information about the local electronic structure of surface atomic configurations with low coordination numbers therefore would be crucial for improving our understanding of their physical properties at the atomic level.

Here we present high-energy resolution core level photoelectron spectroscopy results on $Rh3d_{5/2}$ core level shifts (CLSs), induced by Rh adatoms and ad-dimers, adsorbed on the (100) and (111) Rh surfaces. We have detected the spectral components originating from atoms with many different coordination numbers measuring for the first time the electronic structure of highly under-coordinated atoms, i.e. atoms with nearest neighbour number n equal to 3, 4 and 5. We have also carried out CLSs density functional theory (DFT) calculations for atoms in different geometrical configurations (tracking, in each case, both initial and final state contributions to the shifts). The agreement between calculations and experimental data supports the identification of different spectral components. Furthermore calculations indicate that for Rh final state effects

give a minor contribution to CLSs. We find a linear relationship between CLSs and the energy shifts of the atom projected d-band centre. The latter, in turn, are strongly correlated with atomic coordination numbers, and with interatomic distance changes (ensuing from structure relaxations).

2. Experimental and theoretical methods

The experiments were carried out at the SuperESCA beamline [23, 24] of the synchrotron radiation source ELETTRA. The experimental chamber, with a base pressure of 1×10^{-10} mbar, is equipped with a double pass 96-channel detector electron energy analyser. Clean Rh(100) and Rh(111) samples were prepared following well established procedures [25], consisting of repeated Ar^+ sputtering cycles at room temperature, annealing to 1300 K, oxygen treatments and a final hydrogen reduction. Rh atoms were deposited from the vapour phase via sublimation of a 99.95% purity Rh wire, which was cleaned in ultra-high-vacuum by oxygen and hydrogen treatments at 10^{-7} mbar, followed by annealing at about 1500 K. Surface cleanliness was checked before and after Rh deposition by measuring C1s, O1s, S2p and Si2p XPS signals. Presence of residual hydrogen, which is known to induce new core level components [26, 27], was excluded on the basis of temperature programmed desorption experiments. On the basis of Rh adatom diffusion coefficients data [28] the sample temperature during deposition was maintained at 20 K, in order to exclude adatom surface diffusion and annihilation, by coalescence with steps and/or recombination. In order to minimize the phonon broadening the $Rh3d_{5/2}$ photoemission measurements were also carried out at the same temperature. The overall experimental energy resolution was 60 meV. The spectra were fitted by using a sum of Doniach–Sunjic (DS) [29] functions, convoluted with a Gaussian, which accounts for instrumental resolution and phonon/inhomogeneous broadening. A DS function is characterized by two parameters, the singularity index α, describing the asymmetry due to the final-state screening of the core-hole and the Lorentzian width Γ, due to the finite core-hole lifetime. A linear background was also subtracted.

In order to obtain a more quantitative understanding of the CLSs stemming from the different atomic configurations, we have also performed in-depth DFT calculations. Surface atomic structures, electron densities of states and core-electron eigenvalues were obtained using DFT-ultrasoft pseudo potential calculations [30] based on the local density approximation of the exchange and correlation functionals of Perdew *et al* [31], as implemented in the Quantum-ESPRESSO suite of codes [32]. The Kohn–Sham equations are solved self-consistently using a plane-wave basis set restricted to a kinetic energy cutoff of 30 Ryd. The Brillouin zone integration for the (1×1) cell was approximated through a sampling at a finite number of k points using a $(12 \times 12 \times 2)$ Monkhorst–Pack grid, resulting in 21 special k-points in the irreducible wedge [33]. We have used a Methfessel and Paxton smearing function [34] of order 1 with a width $\sigma = 0.03$ Ryd. The (100) and (111) Rh surfaces were represented by 7-layer repeated slabs with (4×4) in-plane periodicity, one adatom (or dimer) per unit cell (adsorbed on one side of the slab), and a vacuum region equal to five atomic layers; as previously found [35, 36], this vacuum thickness was sufficient to avoid interactions between neighbouring slabs. Final state core level binding energies (BEs) can be accurately computed in the pseudopotential formalism adopted here by describing the excited atom by a pseudopotential generated in the core-excited configuration [37]. In this formulation the core-level BE, including final state effects, is given by the pseudopotential total energy difference supplemented by an additive constant that can be

determined for the isolated atom and cancel out when computing BE differences. Initial state contributions can also be extracted by a frozen-density calculation. Full details of the method used can be found in [35]. The partial density of states we calculate is defined as the projection of the density of states on to the atomic wave-function ϕ_i^{at}:

$$n_i = \sum_n \int_{BZ} \delta(E - E_n(\vec{k}))|\langle \phi_i^{\mathrm{at}} | \psi_n(\vec{k})\rangle|^2 \mathrm{d}\vec{k},$$

where $\psi_n(\mathbf{k})$ is the crystal wavefunction of the nth band at wavevector $\mathbf{k}$. We define the pth moment of the density of states $n_i(E)$ as $\mu_p = \int \varepsilon^p n_i(\varepsilon)\,\mathrm{d}\varepsilon$; μ_0 and μ_1/μ_0 give the total number of states in the band and the centre of gravity position B_{d}, respectively.

3. Experimental results

High-energy resolution Rh3d$_{5/2}$ core-level spectra of the Rh(100) surface with different coverage of deposited Rh atoms are shown in figure 1. In the clean surface spectrum (a), the lower BE component Rh$_{\mathrm{s}}$ originates from first-layer surface atoms, while the higher BE peak is due to the superposition of bulk (at 307.15 eV) and second-layer atoms' contributions (at + 100 meV with respect to the bulk peak), as previously demonstrated [26]. Upon Rh deposition (b), the 3d$_{5/2}$ lineshape clearly changes, as shown by the difference spectrum d$_1$ in figure 1. The growth of new core-level components, both at lower and higher BEs with respect to the Rh$_{\mathrm{s}}$ peak, is compensated by a decrease of the surface component and a drop of the spectral weight at the second-layer peak position, as expected. Longer Rh deposition times (c and d) result in further lineshape modifications, with an enhanced shoulder at low BE and an increased spectral weight in between the bulk and surface peaks.

Spectral multi-peak fitting is a delicate process that requires extreme care for extracting accurate and meaningful quantitative information. For this reason we have used a multi-dimensional least-square analysis of our data. This analysis is needed because of the number of independent components, each defined by different parameters, associated to a specific local atomic configuration. Since the peaks are close to each other, the lineshape parameters of these components can be correlated when performing the fit. In order to rationalize the data analysis procedure, we have mapped the evolution of the chi-square χ^2 as a function of each of the parameters, following the procedure proposed in [38]. The only constraint was to force the lineshape parameters of the adatom- and addimers-induced CLSs (α, Γ and the Gaussian width) to be equal to those of the surface component, while the energy position of each peak was allowed to vary, in order to obtain an estimate of the accuracy of the determined BE ($\pm$30 meV). For example, as shown in figure 2(a) for the Rh(100) spectrum corresponding to a Rh coverage of 0.095 ML, the two-dimensional $\chi^2/\chi^2_{\mathrm{min}}$ contour plot (adatom-induced CLS versus addimer-induced CLS) shows a pronounced and localized minimum, contrary to what observed in the plot (figure 2(b)) relative to the correlation between Gaussian width of the surface peaks versus adatom-induced CLS.

This procedure is based on the analysis of a large set of spectra measured at different photon energies (325–385 eV) and polar emission angles (20°–55° off-normal). Different experimental conditions result in an intensity modulation of the different core level peaks, which facilitates the process of disentangling the different spectral components. The procedure allows (i) to determine

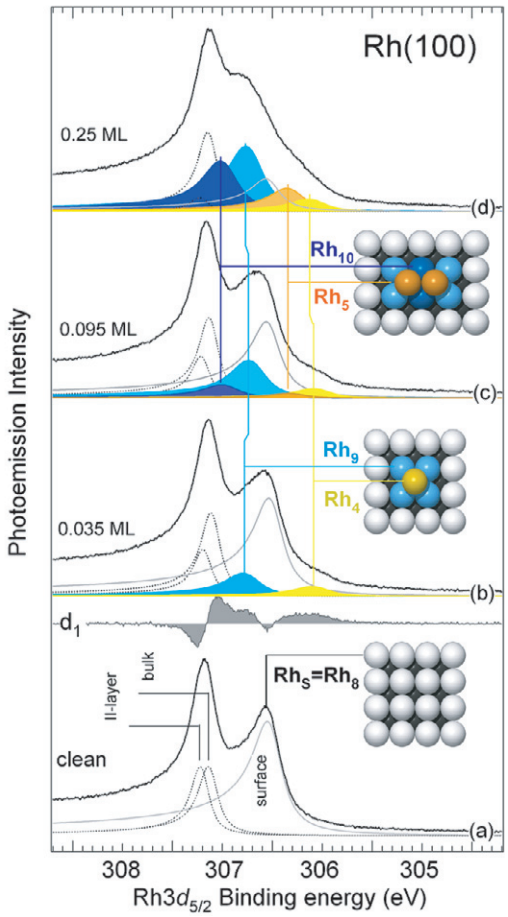

Figure 1. $Rh3d_{5/2}$ core level spectra corresponding to clean (a) and different Rh covered Rh(100) surface (b)–(d). Dashed lines indicate bulk and second layer components, while coloured curves originate from Rh atoms in different local coordination. Individual components are plotted without the linear background. The spectra were acquired at 380 eV photon energy. Polar emission angles was 55° with respect to the surface normal. The curve d_1, obtained as the difference between spectrum b and a, is also reported.

the number of core level components necessary to fit each spectrum, (ii) to extract reliable values of the different CLS components, and (iii) to highlight existing correlations between different fitting parameters. It is important to note that, in general, the intensities of the different spectral components cannot be linked in a straightforward way to the number of emitting atoms, as photoelectron diffraction effects are known to play an important role [39]. This is particularly relevant at low photoelectron kinetic energies [40]–[42], e.g. the ones we used in the present study to achieve high-energy resolution and surface sensitivity.

The low adatom coverage spectrum (figure 1, curve b) can be fitted only by using two extra components at −1030 meV and at −400 meV, with respect to the bulk peak. In the approximation that all the atoms are isolated, we assigned these two components to adatoms (yellow atoms with coordination number $n = 4$) and to surface atoms just below the adatoms (light-blue atoms with $n = 9$). Accordingly, we label these spectral components Rh_4 and Rh_9 respectively; Rh_n

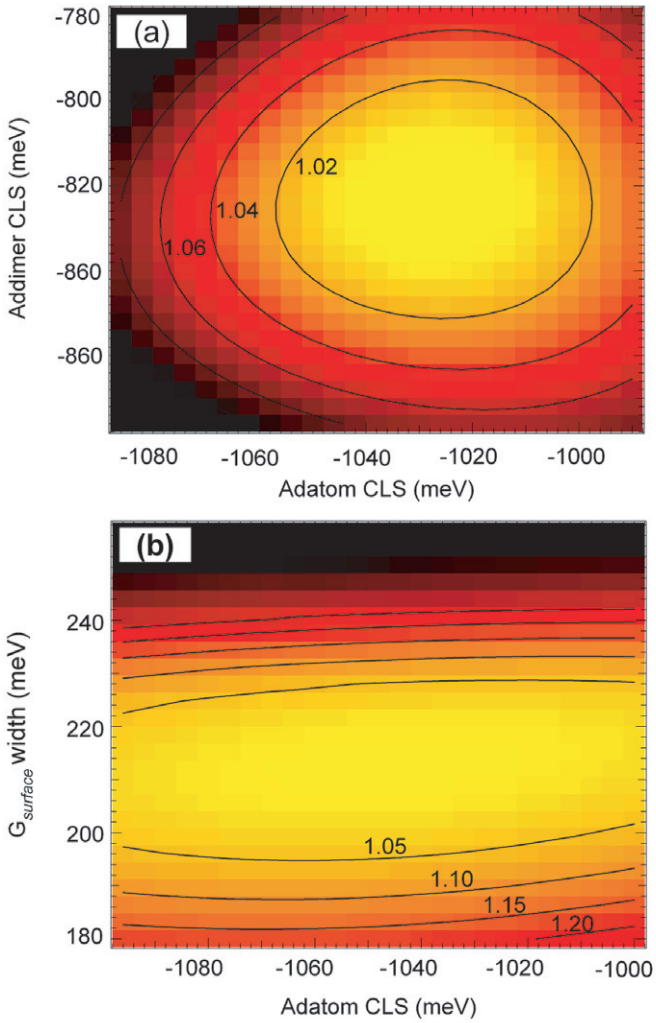

Figure 2. Two-dimensional $\chi^2/\chi^2_{\min}$ contour plots referred to the fit of the Rh(100) spectrum corresponding to a Rh coverage of 0.095 ML. (a) Adatom-induced CLS versus addimer-induced CLS shows a pronounced and localized minimum. (b) On the contrary to the plot in (a) the Gaussian width of the surface peaks parameter does not depend strongly on the adatom-induced CLS.

will be used in the following to indicate the spectral component arising from Rh atoms with coordination number n. The local configuration of atoms that give rise to the Rh_8 ($= Rh_s$) component is the same as for the clean surface atoms; in this case we can therefore use the related intensities as a measure of the atomic densities, as previously successfully done [43]. The 13.8% decrease of the intensity of the Rh_8 component with respect to the clean surface corresponds, in a random distribution model [44], to an overall Rh coverage of 0.035 ML. We have run a simulation of the deposition process, which shows that, under these conditions, 90% of the deposited adatoms are indeed isolated. Using this method, we can evaluate the Rh coverage for longer deposition times. At 0.095 ML (figure 1, curve c), two additional peaks, Rh_5 at -810 meV and Rh_{10} at -145 meV, are needed to obtain a fitting residual with negligible

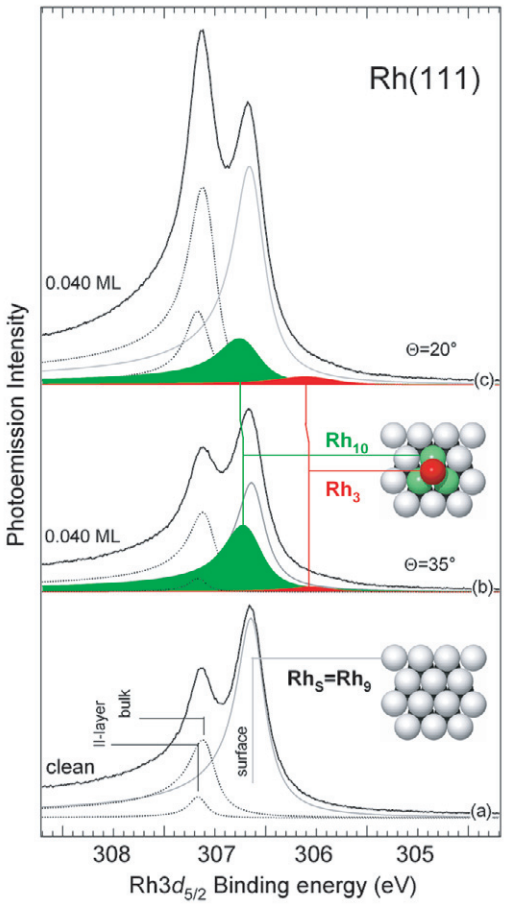

Figure 3. $Rh3d_{5/2}$ core level spectra corresponding to clean (a) and Rh covered Rh(111) surface (b) and (c). Dashed lines indicate bulk and second layer components, while coloured curves originate from Rh atoms in different local coordination. Individual components are plotted without the linear background. The spectra were acquired at 380 eV photon energy. Polar emission angles were 35° (spectra a and b) and 20° (spectrum c), with respect to the surface normal.

modulation. We interpret these additional components as due to the formation of ad-dimers (orange atoms, $n = 5$, and blue atoms,$n = 10$). At this coverage, the Rh_4 and Rh_9 components are still present, albeit the Rh_9 component is slightly shifted to lower BE. At 0.25 ML (figure 1, curve d), the $Rh3d_{5/2}$ spectrum can be satisfactorily fitted with the same components used for 0.095 ML, by allowing the intensities to vary. The analysis shows that the ratio of ad-dimers (Rh_5) to adatoms (Rh_4) populations increases, as expected for higher Rh coverage.

In order to extend our study to the case of very low atomic coordination, we investigated also the Rh(111) surface (figure 3). As previously determined [38] the clean surface (curve a) can be fitted with three components: a lower BE component Rh_s, originating from first-layer surface atoms, and two higher BE components, corresponding to bulk and second-layer atoms' (+88 meV) contributions, similarly to the (100) surface.

At an adatom coverage of 0.040 ML (figure 3, curve b), we find two new core level shifted components: Rh_3 at −1080 meV and Rh_{10} at −380 meV. Rh_3 is assigned to single adatoms

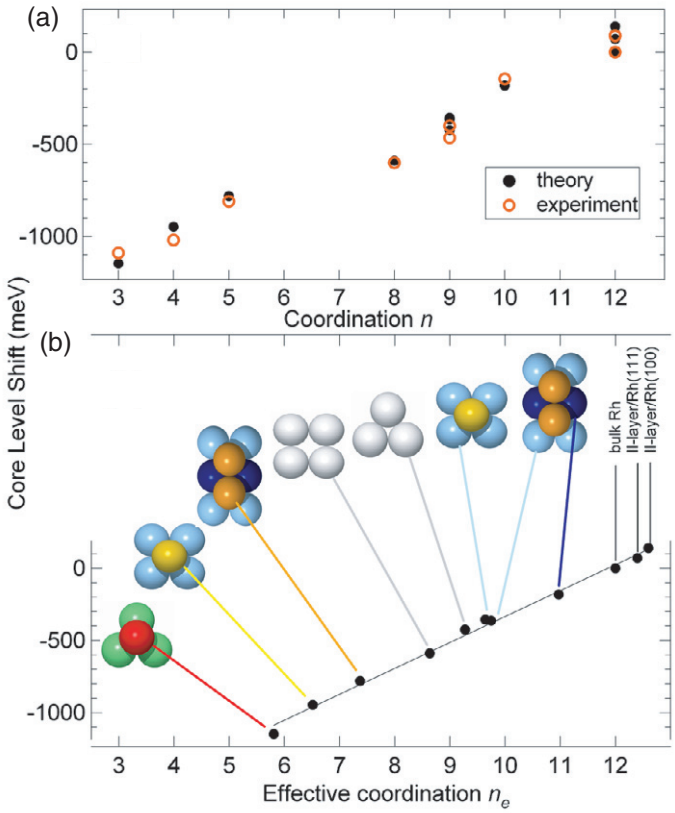

Figure 4. (a) Experimental and calculated CLSs versus nominal atomic coordination number. (b) Calculated CLSs versus effective coordination.

(red atoms) with coordination equal to 3, while Rh_{10} is tentatively interpreted as due to surface atoms (green atoms) nearest-neighbours of the adatoms. The ratio between the Rh_3 and Rh_{10} intensities does not seem to support this interpretation, as it is apparently smaller than the expected value of 1/3 (there are three 'green' atoms for each 'red' atom). However, as stated above, it should be remembered that peak intensities in photoemission spectra are always affected by photoelectron diffraction effects. Therefore it is not possible to draw straightforward conclusions on simple coverage arguments for atoms in inequivalent structural configurations [39]–[42]. An example of this is shown in figure 3, spectrum c, which was measured from the same layer and at the same photon energy of spectrum b, simply changing the polar emission angle ($\Theta = 20^\circ$ instead of 35°). A further complication affecting the Rh_{10} peak is its precise BE position. Indeed, this peak is expected to be originated by two different kind of 'green' atoms that most likely exist on the surface at 20 K, when both fcc (face centred cubic) and hcp (hexagonal close packed) sites can be occupied, giving rise to different core level shifted components. In order to exclude possible artefacts, we therefore excluded the Rh_{10} component from our further consideration.

4. Theoretical results and discussion

In figure 4(a) we plot the experimentally determined CLSs (empty orange circles) together with the calculated ones (filled black circles), which include both initial and

final state effects. Differences are always within error bars (which we estimate to be $\pm$ 30 meV for both experimental and calculated CLS values). For all the structures, core hole screening contributions are of the order of 60 meV (with a scatter of $\pm$30 meV). Therefore, as previously reported for flat surfaces [45, 46], we find that Rh CLSs are dominated by initial state effects. The behaviour of CLSs versus the atomic coordination number shown in figure 4(a) is intriguing. It is approximately linear, as previously observed by Gustafson *et al* [47] for Rh atoms at stepped surface and for coordination $n \geqslant 7$. However, our low coordination data points ($n \geqslant 5$) are clearly positioned on a different line with respect to the higher coordination results ($n \geqslant 8$) and therefore the overall deviations are well outside the error bars. Besides, the different data corresponding to atoms at full ($n = 12$) nominal coordination (bulk and second layer atoms of the (111) and (100) surfaces) differ by $\sim$ 200 meV. A simple electronic structure tight binding model (neglecting final state effects) would predict a linear dependence of CLSs from atomic coordination number.

We conclude that other effects must be contributing to the overall CLSs. A strong interplay between coordination number and local bond strain can be anticipated. Atoms at low coordination sites are subject to large relaxations owing to the more open local structure and reduced symmetry. Indeed, our DFT calculations show that Rh atoms, at low coordination, undergo compressive deformation, relative to the ideal geometry, resulting in a interatomic-distance change of -6 and -7% for adatoms and ad-dimers, respectively. A similar decrease has been found by Richter *et al* [5] for Rh clusters deposited on oxide substrates.

To take into account relaxation effects on the interatomic bond lengths, we introduce an effective coordination of the i site, borrowing ideas from the embedded-atom method (EAM) approach [48]–[50] that successfully models the cohesive energy of metals by considering each atom as embedded in a host whose effect on it is determined by the charge density at the atomic site generated by the host atoms alone. In the practical implementation of EAM this charge density is then approximated by the superposition of atomic charge densities of the host atoms. This definition naturally assigns larger contributions to closer atoms and smoothly phases out farther ones.

We therefore define our effective coordination as $n_{\mathrm{e}}(i) = \sum_j \rho^{\mathrm{at}}_{\mathrm{Rh}}(R_{ij})/\rho^{\mathrm{at}}_{\mathrm{Rh}}(R_{\mathrm{bulk}})$, where the sum is calculated over all the nearest-neighbours j of atom i and $\rho^{\mathrm{at}}_{\mathrm{Rh}}(R)$ is the computed spherical charge density distribution of an isolated Rh atom as function of the distance R from the nucleus, R_{ij} is the distance of the j nearest-neighbour from the i atom and R_{bulk} is the bulk interatomic distance. With this definition the effective coordination is normalized in such a way to agree with the nominal one for atoms in the bulk. Since at the relevant interatomic distance the isolated-atom charge density distribution can very well be described by a simple exponential, of decaying constant b, the expression for the effective coordination further simplifies as $n_{\mathrm{e}}(i) = \sum_j \exp[b(R_{\mathrm{bulk}} - R_{ij})]$.

In figure 4(b) we plot the calculated CLSs as a function of n_{e}. The linear behaviour obtained in this way shows that CLSs strongly depend on both coordination and local interatomic distances, in a combined way which highlights the common origin of the two effects, from the changes in the interatomic matrix elements describing bonds between an atom and its nearest-neighbours. We note that, when plotted against *effective* coordination, CLSs originating from bulk and second layer atoms of both (111) and (100) surfaces (all with nominal coordination $n = 12$) also fall on the same straight line.

Recently, it has been demonstrated that a number of basic local electronic structure indicators, such as the d band centre and d band width, depend on local coordination and

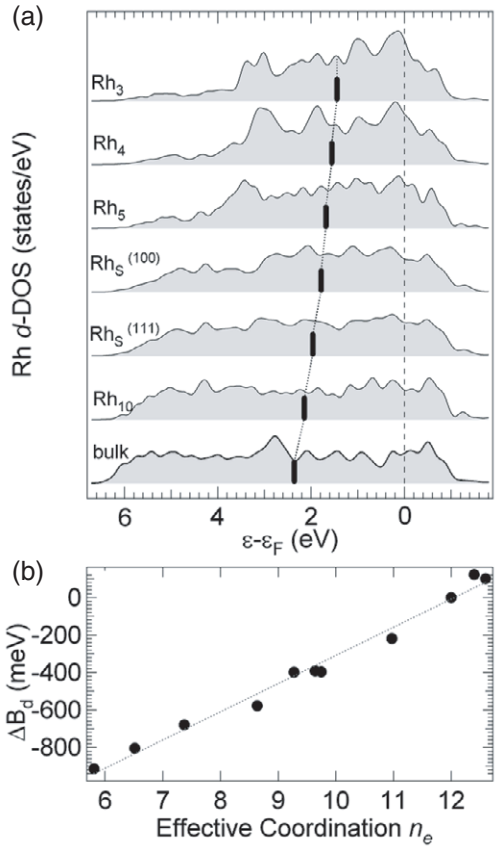

Figure 5. (a) Projected density of states per Rh atom on to the 4d orbitals for atoms in all the considered geometrical configurations. The index n indicates, in each case, the number of nearest–neighbours and the thick lines indicate the d-band centre position B_d. (b) Calculated shift ΔB_d of the d-band centre versus the effective atomic coordination number n_e. Using our binding energy scale ΔB_d is defined as $B_d^{surf} - B_d^{bulk}$.

strain [13], [51]–[53]. In order to evaluate the relationship between CLSs and these relevant chemical and physical quantities, we have calculated the projected density of states (per Rh atom), onto the 4d orbitals, for all the different atomic configurations considered in our study. As shown in figure 5(a), on increasing the coordination number, the projected density of states width increases considerably, while its centre of mass (tick marks) shifts to higher binding energy. In figure 5(b) we plot the shift of the projected d band centre versus the effective coordination number of Rh atoms in the different atomic configurations. The relationship is clearly linear. This implies that the effective coordination number n_e should be considered as an indicator of local electronic structure properties. In the last few years, a number of landmark papers have shown that the d-band centre is also a reliable descriptor of local chemical reactivity [13], [51]–[53]. Therefore our results show that a careful analysis of CLSs provides, for systems where final state effect contributions can be neglected, a spectroscopic measure of chemical reactivity changes, at the atomic level.

5. Conclusions

We have shown that high-resolution core level spectroscopy can be successfully used for investigating local chemical and physical properties of under-coordinated surface atoms. In particular we have detected, for the first time, the spectral contribution of atoms at the lowest coordination numbers ($n = 3, 4$ and 5). We have also carried out in-depth DFT calculations, which fully confirm our interpretation of the experimental data. Besides, the calculations have allowed us to introduce the effective coordination number n_e, which has been shown to be a reliable descriptor of local electronic structure at the atomic level. On the basis of these results, we believe that CLSs can become a powerful tool for characterizing nanostructured surfaces.

Acknowledgments

We acknowledge financial support from the MIUR under the programs PRIN2003 and FIRB2001. GZ acknowledges the ICTP for financial support.

References

[1] Barth J V, Costantini G and Kern K 2005 *Nature* **437** 671
[2] Bell A T 2003 *Science* **299** 1688
[3] Wertheim G K, DiCenzo S B and Buchanan D N E 1986 *Phys. Rev.* B **33** 5384
[4] Wertheim G K 1989 *Z. Phys.* D **12** 319
[5] Richter B, Kuhlenbeck K, Freund H-J and Bagus P S 2004 *Phys. Rev. Lett.* **93** 26805
[6] Zambelli T, Wintterlin J, Trost J and Ertl G 1996 *Science* **273** 5282
[7] Xu Y and Mavrikakis M 2003 *J. Phys. Chem.* B **107** 9298
[8] Zhang C, Liu Z P and Hu P 2001 *J. Chem. Phys.* **115** 609
[9] Liu Z, Hu P and Alavi A 2001 *J. Am. Chem. Soc.* **124** 14770
[10] Liu Z P, Jenkins S J and King D A 2003 *J. Am. Chem. Soc.* **125** 14660
[11] Liu Z P and Hu P 2003 *J. Am. Chem. Soc.* **125** 1958
[12] Zubkov T, Morgan G A and Yates J T Jr 2002 *Chem. Phys. Lett.* **362** 181
[13] Mavrikakis M, Hammer B and Nørskov J K1998 *Phys. Rev. Lett.* **81** 2819
[14] Buatier de Mongeot F, Toma A, Molle A, Lizzit S, Petaccia L and Baraldi A 2006 *Phys. Rev. Lett.* **97** 56103
[15] Silvestri W, Graham A P and Toennies J P 1998 *Phys. Rev. Lett.* **81** 1034
[16] Tromp R M and Toennies J P 1998 *Phys. Rev. Lett.* **81** 1050
[17] Lin N, Payer D, Dmitriev A, Strunskus T, Wölll C, Barth J V and Kern K 2005 *Angew. Chem. Int. Edn Engl.* **44** 1488
[18] Abbet S, Sanchez A, Heiz U, Schneider W, Ferrari D, Pacchioni GA M and Rosch N 2000 *J. Am. Chem. Soc.* **122** 3453
[19] Abbet S, Heiz U, Häkkinen H and Landman U 2001 *Phys. Rev. Lett.* **86** 5950
[20] Kokalj A, Bonini N, Sbraccia C, de Gironcoli S and Baroni S 2004 *J. Am. Chem. Soc.* **126** 16732
[21] Kokalj A, Bonini N, de Gironcoli S, Sbraccia C, Fratesi G and Baroni S 2006 *J. Am. Chem. Soc.***128** 12448
[22] Zhang C and Hu P 2001 *J. Chem. Phys.* **116** 4281
[23] Baraldi A, Barnaba M, Brena B, Cocco D, Comelli G, Lizzit S, Paolucci G and Rosei R 1995 *J. Electron Spectrosc. Relat. Phenom.* **76** 145
[24] Baraldi A, Comelli G, Lizzit S, Kiskinova M and Rosei R 2003 *Surf. Sci. Rep.* **49** 169
[25] Baraldi A, Dhanak V R, Comelli G, Prince K C and Rosei R 1997 *Phys. Rev.* B **56** 10511
[26] Vesselli E, Baraldi A, Bondino F, Comelli G, Peressi M and Rosei R 2004 *Phys. Rev.* B **70** 115404
[27] Weststrate C J, Baraldi A, Rumiz L, Lizzit S, Comelli G and Rosei R 2004 *Surf. Sci.* **486** 566

[28] Stolt K, Graham W R and Ehrlich W R 1976 *J. Chem. Phys.* **65** 3206
[29] Doniach S and Sunjic M1970 *J. Phys. C: Solid State Phys.* **3** 185
[30] Vanderbilt D 1990 *Phys. Rev.* B **41** 7892
[31] Perdew J P and Zunger A 1981 *Phys. Rev.* B **23** 5048
[32] Baroni S, de Gironcoli S, Dal Corso A and Giannozzi P online at http://www.quantum-espresso.org
[33] Monkhorst H J and Pack J D 1976 *Phys. Rev.* B **13** 5188
[34] Methfessel M and Paxton A T 1989 *Phys. Rev.* B **40** 3616
[35] Bianchettin L, Baraldi A, de Gironcoli S, Vesselli E, Lizzit S, Petaccia L, Comelli G and Rosei R 2006 *Phys. Rev.* B **74** 45430
[36] Bianchettin L, Baraldi A, Vesselli E, de Gironcoli S, Lizzit S, Petaccia L, Comelli G and Rosei R 2007 *J. Phys. Chem.* C **111** 4003
[37] Pehlke E and Scheffler M 1993 *Phys. Rev. Lett.* **71** 2338
[38] Baraldi A, Lizzit S, Novello A, Comelli G and Rosei R 2003 *Phys. Rev.* B **67** 205404
[39] Woodruff D P and Bradshaw A M 1994 *Rep. Prog. Phys.* **57** 1029
[40] Lizzit S, Pohl K, Baraldi A, Comelli G, Fritzsche V, Plummer E W, Stumpf R and Hofmann Ph 1998 *Phys. Rev. Lett* **81** 3271
[41] Baraldi A, Lizzit S, Comelli G, Goldoni A, Hofmann Ph and Paolucci G 2000 *Phys. Rev.* B **61** 4534
[42] Lizzit S *et al* 2001 *Phys. Rev.* B **63** 205419
[43] Baraldi A, Lizzit S, Comelli G, Kiskinova M, Rosei R, Honkala K and Nørskov J K 2004 *Phys. Rev. Lett.* **93** 46101
[44] Chen M S, Kumar D, Yi C W and Goodman D W 2005 *Science* **310** 291
[45] Andersen J N, Hennig D, Lundgren E, Methfessel M, Nyholm R and Scheffler M 1994 *Phys. Rev.* B **50** 17525
[46] Ganduglia-Pirovano M V, Scheffler M, Baraldi A, Lizzit S, Comelli G, Paolucci G and Rosei R 2001 *Phys. Rev.* B **63** 205415
[47] Gustafson J, Borg M, Mikkelsen A, Gorovikov S, Lundgren E and Andersen J N 2003 *Phys. Rev. Lett.* **91** 56102
[48] Daw M S and Baskes M I 1983 *Phys. Rev. Lett.* **50** 1285
[49] Daw M S and Baskes M I 1984 *Phys. Rev.* B **29** 6443
[50] Foiles M S and Baskes M I 1986 *Phys. Rev.* B **33** 7983
[51] Hammer B and Nørskov J K 2000 *Adv. Catal.* **45** 71
[52] Hammer B, Morikawa Y and Nørskov J K 1996 *Phys. Rev. Lett.* **76** 2141
[53] Kitchin J R, Nørskov J K, Barteau M A and Chen J G 2004 *Phys. Rev. Lett.* **93** 156801